

Argonne National Laboratory
A FORTRAN PROGRAM TO ANALYZE
MASS SPECTROMETER ION OPTICS

by

Kurt Kaiser

LEGAL NOTICE

This report was prepared as an account of Government sponsored work. Neither the United States, nor the Commission, nor any person acting on behalf of the Commission:

A. Makes any warranty or representation, expressed or implied, with respect to the accuracy, completeness, or usefulness of the information contained in this report, or that the use of any information, apparatus, method, or process disclosed in this report may not infringe privately owned rights; or

B. Assumes any liabilities with respect to the use of, or for damages resulting from the use of any information, apparatus, method, or process disclosed in this report.

As used in the above, "person acting on behalf of the Commission" includes any employee or contractor of the Commission, or employee of such contractor, to the extent that such employee or contractor of the Commission, or employee of such contractor prepares, disseminates, or provides access to, any information pursuant to his employment or contract with the Commission, or his employment with such contractor.

TABLE OF CONTENTS

ABSTRACT

INTRODUCTION

INPUT DATA

PROGRAM OUTPUT

SAMPLE PROBLEM

REMARKS

THE FORTRAN PROGRAM

REFERENCES

ARGONNE NATIONAL LABORATORY
9700 South Cass Avenue
Argonne, Illinois 60440

A FORTRAN PROGRAM TO ANALYZE
MASS SPECTROMETER ION OPTICS

by

Kurt Kaiser

Chemistry Division

August 1964

Operated by The University of Chicago
under
Contract W-31-109-eng-38
with the
U. S. Atomic Energy Commission

TABLE OF CONTENTS

<u>No.</u>	<u>Title</u>	<u>Page</u>
	ABSTRACT	4
	INTRODUCTION	4
	INPUT DATA	5
	PROGRAM OUTPUT	9
	SAMPLE PROBLEM	12
	REMARKS	16
	THE FORTRAN PROGRAM	17
	REFERENCES	24

LIST OF TABLES

<u>No.</u>	<u>Title</u>	<u>Page</u>
I.	Input Data Card Format	5
II.	Input Data for Sample Problem	12
III.	Sample Problem Output	14
IV.	Fortran Program Listing	17

LIST OF FIGURES

<u>No.</u>	<u>Title</u>	<u>Page</u>
1.	Figure Showing the Trajectories of Two Ions through an Electromagnetic Sector Field	5
2.	Radial Section of a Magnetic Sector	6
3.	Toroidal Electrostatic Sector Field	6
4.	A Tandem Sector Field System	8
5.	Figure Illustrating the Direction and Energy Focusing Curves and the Angles these Curves Make with the Optic Axis	11
6.	100 in. Radius Double Focusing Mass Spectrometer	12
7.	First-order Approximation to the Ion Trajectories for the Argonne 100-in. Mass Spectrometer	15
8.	Fortran Program Flow Chart	18

LIST OF TABLES

<u>No.</u>	<u>Title</u>	<u>Page</u>
I.	Input Data Card Format	8
II.	Input Data for Sample Problem	13
III.	Sample Problem Output	14
IV.	Fortran Program Listing	19

A FORTRAN PROGRAM TO ANALYZE MASS SPECTROMETER ION OPTICS

by

Kurt Kaiser

ABSTRACT

A Fortran program is described for the computation of ion-optical aberration coefficients through second order for any number of tandem electric and magnetic sector fields, such as those used in multistaged mass spectrometers. Also computed are the image positions and their magnifications, the system mass dispersion, and the inclinations of the direction- and energy-focusing planes with respect to the optic axis.

INTRODUCTION

Since 1950 extensive studies have been made of the ion-optical properties of tandem electric and magnetic sector fields by Johnson and Nier,⁽¹⁾ Voorhies,⁽²⁾ Hintenberger and König,⁽³⁾ Ewald and Liebl,⁽⁴⁾ Tasman, Boerboom, and Wachsmuth,⁽⁵⁾ and others. These studies formed the basis for the computer program described herein, although other results were derived when needed.

This program considers ions having the following initial conditions different from those of ions which traverse the systems optic axis (see Fig. 1):

- (1) an initial angle to the optic axis

α in the radial direction;

α_z in the axial direction;

- (2) a different velocity or energy

$V = V_0(1 + \beta)$ or

$E = E_0(1 + \eta)$;

- (3) a different mass

$M = M_0(1 + \gamma)$;

- (4) an initial displacement to the optic axis

δ in the radial direction;

δ_z in the axial direction.

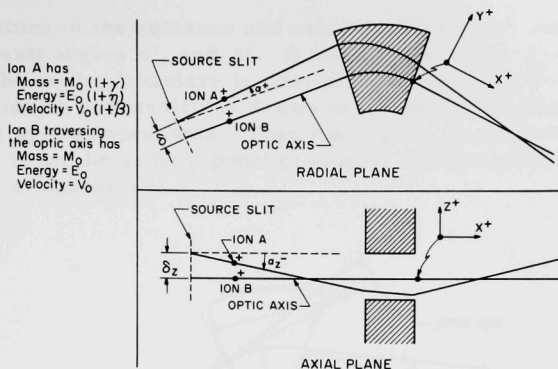


Fig. 1. Figure Showing the Trajectories of Two Ions through an Electromagnetic Sector Field. The initial displacement of ion A to the optic axis is resolved into the radial component δ and an axial component δ_z . Also, its initial direction to the optic axis is resolved into radial and axial components α and α_z , respectively.

The program calculates ion trajectories as functions of α , β , γ , δ , α_z , and δ_z . In the radial plane the trajectories are given as power series to second-order terms, and in the axial direction to first-order terms. In field-free regions the trajectories are straight lines given directly by the program output. Points along the trajectories in the sector fields can be found by subdividing the field into a number of tandem sector fields, zero distance apart, and reading out computed data for each edge of the subfields.

The electric sectors may have curved boundaries and toroidal shape, which includes cylindrical and spherical analyzers as special cases. The magnetic fields are assumed homogeneous, but can have non-normal entrance and exit, as well as circularly curved boundaries.

INPUT DATA

The input data to this program are punched on cards, one card for each field in the system. For convenience these data are divided into three types, each of which is discussed below.

TYPE I DATA: A set of parameters for each field specifying its configuration:

(1) For a homogeneous magnetic field, as shown in Fig. 2, the relevant parameters are the field radius r_m , the beam-deflection angle ϕ_m , the

radii of curvature of the entrance and exit boundaries, R' , and R'' , and the entrance and exit angles ϵ' , and ϵ'' . A radius of curvature is positive (negative) if the sector boundary is convex (concave) towards the field-free region. Consider a perpendicular drawn to the sector boundary where it intersects the system optic axis. Then the angle ϵ is positive (negative) if the optic axis is on the same (opposite) side of this perpendicular as the sector center of curvature.

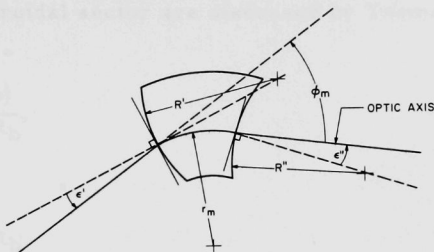


Fig. 2. Radial Section of a Magnetic Sector Field.
In this figure R' is positive, R'' is negative,
 ϵ' is positive, and ϵ'' is negative.

(2) For a toroidal electric field, as shown in Fig. 3, the parameters are the radius r_e , described by the optic axis, the beam-deflection angle ϕ_e , the radii of curvature of the entrance and exit boundaries, R_I and R_{II} , and two parameters, c and R'_e , describing approximately the electric field in the neighborhood of the optic axis. Again, the radius of curvature of a boundary is positive (negative) if the sector boundary is convex (concave) towards the field-free region.

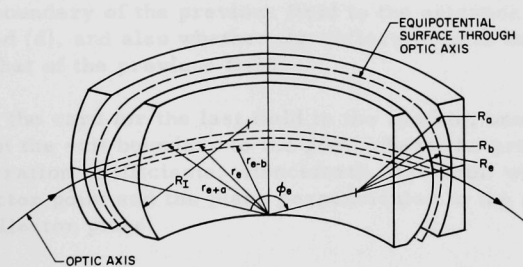


Fig. 3. Toroidal Electrostatic Sector Field.
The entrance boundary has a positive
curvature with its center of curvature
in the Median plane.

The two parameters c and R'_e are defined as follows:

$$c = r_e / R'_e,$$

and

$$R'_e = \left(\frac{\partial R}{\partial r} \right)_{r=r_e, z=0},$$

where R is the radius of curvature of an equipotential surface near the optic axis and the other symbols are as defined in Fig. 3. The values of c and R'_e for a general toroidal sector are discussed by Tasman⁽⁶⁾ and Albrecht.⁽⁷⁾ To first order,

$$c = \frac{r_e(a+b)}{bR_a + aR_b},$$

and

$$R'_e = \frac{R_a - R_b}{a + b}.$$

Two special types of toroidal electric fields are frequently used: the cylindrical analyzer which has $c = 0$ and $R'_e = 1$, and the spherical analyzer which has $c = 1$ and $R'_e = 1$.

TYPE II DATA: A set of parameters describing the relation of each field to its neighbors (see Fig. 4):

(1) On the card for the first field, one enters the distance from the source slit to the first field entrance boundary (ℓ').

(2) On the rest of the cards for the system, one enters the distance from the exit boundary of the previous field to the entrance boundary of the field considered (d), and also whether the deflection is in the same or opposite sense as that of the previous field.

(3) On the card for the last field in the system, one enters the distance (ℓ'') from the exit boundary to the point where the program is to calculate the aberration coefficients. Henceforth, this point will be referred to as the collector point and the plane perpendicular to the optic axis at this point as the collector plane.

(4) On each field card enter the sequence number of each field along with the total number of fields in the system.

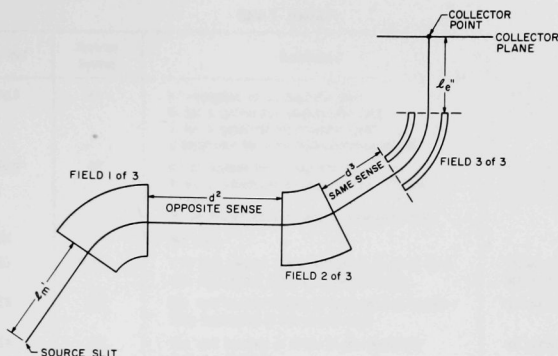


Fig. 4. A Tandem Sector Field System

TYPE III DATA: Digits for controlling the following program options:

- (1) For a single symmetric field, the program can calculate both the entrance and the exit distances (ℓ' and ℓ''), so the point of first-order angle (α) focus is the collector point.
- (2) For any system of fields, the program can calculate the distance (ℓ'') from the last field to the point of first-order angle (α) focus and use it as the collector point.
- (3) The aberration coefficients can be calculated in terms of energy differences η rather than velocity differences β .
- (4) The coefficient and ray trace arrays, described under output, may be read out if desired.

A detailed listing of the data card format is given in Table I.

Table I
INPUT DATA CARD FORMAT

Card Columns	Format	Fortran Symbol	Explanation	Punched on
1-6	F6.0	Q	Field deflection angle in degrees (θ_e or θ_m)	all cards.
7-12	F6.0	R	Field radius (r_e or r_m)	all cards.
13-18	F6.0	DA	The distance from the source slit to the first field (ℓ_e' or ℓ_m')	card for the first field only. Not necessary at all if 1 is punched in CC77.
19-24	F6.0	DB	The distance from the previous field to the present field (d)	all cards except the one for the first field.
25-30	F6.0	DC	The distance from the last field to the point where an aberration coefficient summary is desired (collector point) (ℓ_e'' or ℓ_m'')	card for the last field only. Not necessary at all if 1 is punched in CC76.
31-36	F6.0	R1	The radius of curvature of the entrance field boundary (R' or R_I)	all cards that do not have a 2 or 3 punched in CC74.
37-42	F6.0	R2	The radius of curvature of the exit field boundary (R'' or R_{II})	all cards that do not have a 2 or 4 punched in CC74.

Table I (Contd.)

Card Columns	Format	Fortran Symbol	Explanation	Punched on
43-48	F6.0	E1	ϵ' in degrees for a magnetic field 0. for a cylindrical electrostatic field 1. for a spherical electrostatic field c parameter for a toroidal electrostatic field	all cards except those magnetic field cards that have $\epsilon' = 0$.
49-54	F6.0	E2	ϵ'' in degrees for a magnetic field 1. for a cylindrical or spherical electrostatic field R_0 parameter for a toroidal electrostatic field	all cards except those magnetic field cards that have $\epsilon'' = 0$.
55-59	5X		Not used	
60	I1	I9	1 in this column if the printer is to bring up a new page before doing any more printing	those cards where this option is desired.
61-66	I6	K1	The field number (fields to be numbered sequentially beginning at the source end)	all cards.
67-72	I6	K2	The total number of fields in the particular system considered	all cards.
73	I1	I1	1 for a magnetic field, blank for an electric field	all cards.
74	I1	I2	1 if R1 and R2 (CC 31-42) are both <u>not</u> equal to infinity. 2 if R1 and R2 (CC 31-42) are both equal to infinity. 3 if R1 (CC 31-36) is equal to infinity and R2 (CC 37-42) is <u>not</u> equal to infinity. 4 if R1 (CC 31-36) is <u>not</u> equal to infinity and R2 (CC 37-42) is equal to infinity.	all cards.
75	I1	I3	1 if the deflection is in the opposite sense as the previous field, blank if it is in the same sense	all cards except the one for the first field.
76	I1	I4	1 if the program is to calculate the distance from the last field to the image plane which gives first-order angle focusing - this distance will be printed out (labeled DC) and used in subsequent calculations.	card for the last field when this option is desired.
77	I1	I5	1 if the program is to calculate the distance from the source to the first field - this feature can be used for a <u>single</u> symmetric field only.	field card on which this option is wanted.
78	I1	I6	1 if the aberrations are to be obtained in the η (energy) representation, blank for aberrations in the β (velocity) representation	all cards, blanks or ones must be used consistently throughout a system.
79	I1	I7	1 for the coefficient print feature	card for field for which this option is desired.
80	I1	I8	1 for the ray trace print feature	card for field for which this option is desired.

Notes:

1. CC abbreviation for card column(s).
2. The distances required above may be measured in any consistent unit.

PROGRAM OUTPUT

For each field-free space this program calculates the radial displacement y to second order and the axial displacement z to first order as a function of α , β , γ , δ , α_z , and δ_z . This is accomplished by calculating certain constants for each field, then altering the aberration coefficients by use of these constants with a subprogram.

After each field is calculated the coefficients may be read out through a program option. This feature is called the coefficient print.

If this option is elected, thirty-six coefficients are read out for each field, in the order C_1 to C_{18} , then D_1 to D_{18} . This output is labeled by C followed by the field number. Specifically, the C's and D's are defined by the following equations, where the superscript

1 refers to the first field of a system,

ℓ refers to the last field of a system, and

N refers to the Nth field of a system:

$$\begin{aligned}
 Y^N = & r^N \left[C_1^N \alpha + C_2^N \beta + C_3^N \gamma + C_4^N \left(\frac{\delta}{r^1} \right) + C_7^N \alpha^2 + C_8^N \alpha \beta + C_9^N \beta^2 + C_{10}^N \alpha \gamma + C_{11}^N \beta \gamma + C_{12}^N \gamma^2 \right. \\
 & + C_{13}^N \alpha \left(\frac{\delta}{r^1} \right) + C_{14}^N \beta \left(\frac{\delta}{r^1} \right) + C_{15}^N \left(\frac{\delta}{r^1} \right)^2 + C_{16}^N \alpha_z^2 + C_{17}^N \alpha_z \left(\frac{\delta}{r^1} \right) + C_{18}^N \left(\frac{\delta}{r^1} \right)^2 \Big] \\
 & + X^N \left[D_1^N \alpha + D_2^N \beta + D_3^N \gamma + D_4^N \left(\frac{\delta}{r^1} \right) + D_7^N \alpha^2 + D_8^N \alpha \beta + D_9^N \beta^2 + D_{10}^N \alpha \gamma + D_{11}^N \beta \gamma \right. \\
 & + D_{12}^N \gamma^2 + D_{13}^N \alpha \left(\frac{\delta}{r^1} \right)^2 + D_{14}^N \beta \left(\frac{\delta}{r^1} \right) + D_{15}^N \left(\frac{\delta}{r^1} \right)^2 + D_{16}^N \alpha_z^2 + D_{17}^N \alpha_z \left(\frac{\delta}{r^1} \right) + D_{18}^N \left(\frac{\delta}{r^1} \right)^2 \Big], \\
 Z^N = & r^N \left[C_5^N \alpha_z + C_6^N \left(\frac{\delta}{r^1} \right) \right] + X^N \left[D_5^N \alpha_z + D_6^N \left(\frac{\delta}{r^1} \right) \right];
 \end{aligned}$$

In these equations r is a field radius, X^N is the distance along the optic axis measured from the exit boundary of the Nth field, and Y^N and Z^N are the displacements measured in a plane located at X^N perpendicular to the optic axis. Note that Y^N is positive on the opposite side of the optic axis from the field center of curvature, Z^N is positive if above the optic axis, and (X^ℓ, Y^ℓ, Z^ℓ) are the coordinates in image space.

At this time twelve first-order coefficients: W_1 to W_6 for the entrance boundary, and W_1 to W_6 for the exit boundary, may be printed out. These twelve are labeled by R followed by the field number. This option is called the ray trace. The W's are defined by the equations

$$Y^N = W_1^N \alpha + W_2^N \beta + W_3^N \gamma + W_4^N \delta$$

and

$$Z^N = W_5^N \alpha_z + W_6^N \delta_z.$$

Just before the program summary a line labeled RS is read out, which contains W_1 to W_6 calculated at the collector point.

After the last field calculation has been completed, the program begins a summary calculation. This summary includes the aberration coefficients for the collector plane and other constants of the system. Eighteen coefficients B_1 to B_{18} , labeled S1, are read out. They are

defined by the equations

$$\begin{aligned} \frac{Y^N}{r^\ell} = & B_1\alpha + B_2\beta + B_3\gamma + B_4\left(\frac{\delta}{r^1}\right) + B_7\alpha^2 + B_8\alpha\beta + B_9\beta^2 + B_{10}\alpha\gamma + B_{11}\beta\gamma + B_{12}\gamma^2 \\ & + B_{13}\alpha\left(\frac{\delta}{r^1}\right) + B_{14}\beta\left(\frac{\delta}{r^1}\right) + B_{15}\left(\frac{\delta}{r^1}\right)^2 + B_{16}\alpha_z^2 + B_{17}\alpha_z\left(\frac{\delta_z}{r^1}\right) + B_{18}\left(\frac{\delta_z}{r^1}\right)^2 \end{aligned}$$

and

$$\frac{Z^N}{r^\ell} = B_5\alpha_z + B_6\left(\frac{\delta_z}{r^1}\right).$$

Following the S1 readout is the last output record, labeled S2, which contains the following six constants in order;

- (1) the position of the axial focusing plane, i.e., the distance X^ℓ to the point where $B_5 = 0$;
- (2) the system mass dispersion per $\Delta M/M$;
- (3) the radial image magnification (measured at the point of α focus, i.e., where $B_1 = 0$);
- (4) the axial image magnification (measured at the point of α_z focus, i.e., where $B_5 = 0$);
- (5) the angle ψ_α that the direction-focusing curve makes with the optic axis;
- (6) the angle ψ_β (or ψ_η) that the velocity (energy)-focusing curve makes with the optic axis.

The angles ψ_α and ψ_β (or ψ_η) (see Fig. 5) are defined as follows: the locus of points of direction or α focus described as an ion mass or γ is varied will be a surface in image space. The intersection of this surface with the system median plane is the direction-focusing curve χ_α . The slope, in degrees, of the tangent to χ_α at its intersection with the optic axis is ψ_α . The X^ℓ coordinate of this point is the one for which $B_1 = 0$. In a completely analogous manner, the velocity or energy parameters χ_β and ψ_β (or χ_η and ψ_η) may be defined. The X^ℓ coordinate for the intersection of χ_β or χ_η with the optic axis is that value which makes $B_2 = 0$. The angle ψ_β (or ψ_η) is of most interest for systems which are "double focusing," that is, where B_1 and B_2 both equal zero for the same value of X^ℓ .

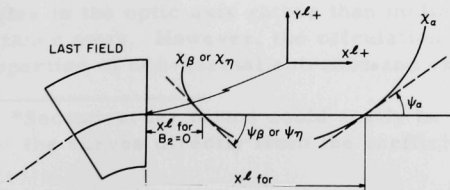


Fig. 5

Figure Illustrating the Direction and Energy Focusing Curves and the Angles These Curves Make with the Optic Axis. In this figure ψ_α is positive and ψ_β is negative.

SAMPLE PROBLEM

As an example of the use of this program consider the Argonne 100-in. mass spectrometer, shown pictorially in Fig. 6. This instrument consists of a 100-in.-radius, 75° spherical electrostatic analyzer, followed by a 100-in.-radius, 110° magnetic analyzer.

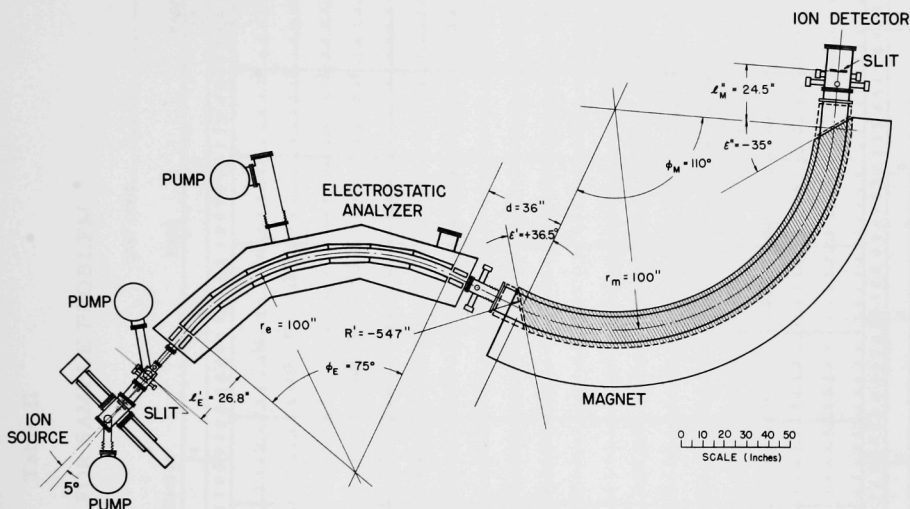


Fig. 6. 100-in. Radius Double Focusing Mass Spectrometer

The parameters to be used in this example were read off Fig. 6 and punched on data cards as in Table II. The program output listing is shown in Table III, in which the second S1 and S2 outputs are for the energy (η) rather than the velocity (β) representation used in the preceding output records.

The ray trace feature was used to calculate the curves plotted in Figs. 7A and 7B. For this calculation the electric and magnetic sectors were each divided into ten subfields zero distance apart. The ray trace output for these twenty fields gave enough points to plot the curves. This output takes into account first-order* terms only, i.e., rays an infinitesimal distance away from the optic axis. In the figures the dimensions measured perpendicular to the optic axis can be considered greatly magnified. For this reason the magnetic sector boundaries are shown at right angles to the optic axis rather than inclined as they look to rays at a finite distance away. However, the calculation does take into account the focal properties of non-normal entrance and exit from the magnetic field.

*Second-order terms could easily be taken into account by calculating the curves directly from the coefficient print feature.

INPUT DATA FOR SAMPLE PROBLEM

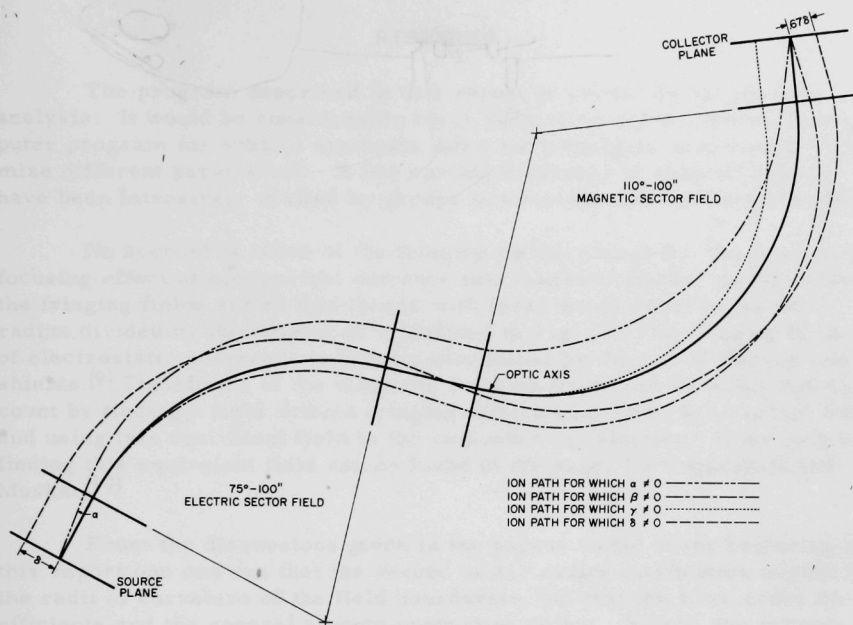
COST CODE _____

[illegible]

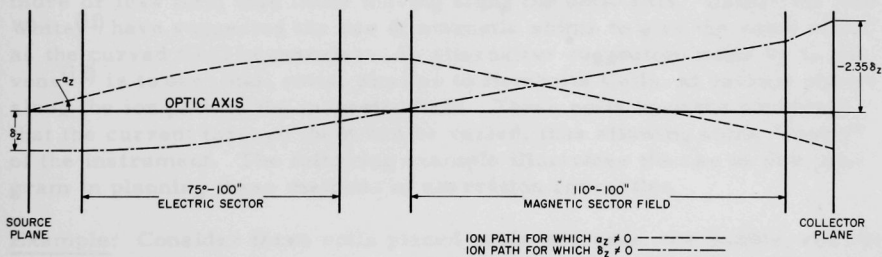
Table III

SAMPLE PROBLEM OUTPUT

C 1	1.03528933 1.03528933 -0.02614593 -0.96602072 0.76733677 -0.00004911 -0.00004911 -0.03407404 -1.25884443 0.99997631	1.48236198 0.25881901 0.00000000 3.73205088 0.09591587 1.93185167 -0.96592584 0.00000000 2.93185155 -0.23296295	0.00000000 -0.00004912 0.00000000 -0.93301272 0.00000000 -1.03534018 0.00000000 -0.24999997	0.25881901 3.86389310 0.00000000 -0.26774917 -0.96592584 3.03542511 0.00000000 0.03472601
R 1	26.80000000 26.80000000 0.00000000	0.00000000 1.00000000 0.25881901	0.00000000 103.52893304 103.52893304	1.00000000 148.23619794 0.25881901
C 2	-0.36573166 -0.43555374 -10.52564577 1.82385587 -2.26343107 1.49091663 -1.07108789 0.81198440 -3.41156817 2.62351919	-1.24278774 -1.81704510 -0.70047860 -2.17157112 -0.32902210 5.06829209 -2.17244144 -0.74548292 9.73563290 -0.21561004	0.67101010 0.19775253 -2.61798160 0.57892024 -0.00000004 -0.60531209 -1.56822031 -1.72109583	0.93908818 -9.78742093 -0.16775250 -0.33628085 -1.09397747 12.63628107 0.00000003 -0.33287348
R 2	-103.52716495 103.52716495 67.10100965	-217.78285810 -0.08891429 0.93908818	-0.00000000 -36.57316597 -43.55537433	0.08891429 -124.27877381 -1.81704510
RS	-0.04570846 -69.79702763	-0.10561756 -2.34929325	67.10100859	0.67106371
S1	-0.00045708 -0.69797028 -10.32670959 0.98802167 -1.62066887	-0.00105618 -2.34929325 -0.88312192 0.21365894 -0.38184657	0.67101009 0.04945107 -3.00219557 0.15725176	0.67106371 -6.69153207 -0.16775250 -0.41783494
S2	-40.66461282 48.56350975	67.10100859 48.56285248	0.67072831	-0.93363020
S1	-0.00045708 -0.69797028 -2.66548765 0.98802167 -1.62066887	-0.00052809 -2.34929325 -0.88312192 0.10682947 -0.38184657	0.67101009 0.04945107 -1.50109779 0.15725176	0.67106371 -3.34576604 -0.16775250 -0.41783494
S2	-40.66461282 48.56350975	67.10100859 48.56285248	0.67072831	-0.93363020



A. Radial Plane



B. Axial Plane

Fig. 7. First-order Approximation to the Ion Trajectories for the Argonne 100-in. Mass Spectrometer. These plots were found by use of the ray trace feature of the program. Note that the distance in the radial and axial directions are shown greatly magnified.

REMARKS

The program described in this report is primarily for system analysis. It would be considerably more difficult to write a general computer program for system synthesis since each designer may wish to optimize different parameters. A few special syntheses of general interest have been intensively studied by groups in Germany and the Netherlands.⁽⁸⁾

No account is taken of the fringing fields, except for the Z or axial focusing effect of non-normal entrance into magnetic fields. In this case the fringing fields act as thin lenses with focal length equal to the field radius divided by the tangent of ϵ (defined in Fig. 2). The fringing field of electrostatic analyzers is usually eliminated by the use of Herzog end shields.⁽⁹⁾ The effects of the magnetic fringing fields can be taken into account by finding a field without fringing effects equivalent to an actual field and using this equivalent field in the computer calculations. Some help in finding this equivalent field can be found in the paper by Coggeshall and Muskat.⁽¹⁰⁾

From the discussions given in the papers listed at the beginning of this report one can see that the second-order radial coefficients depend on the radii of curvature of the field boundaries, but that the first-order coefficients and the general system properties do not. In fact, the second-order coefficients are linear functions of the reciprocals of these radii. With curved field boundaries, the ions traveling off the optic axis see slightly more or less field than those moving along the optic axis. Balestrini and White⁽¹¹⁾ have suggested the use of magnetic shims to give the same effect as the curved field boundaries. An alternative suggestion made by C. Stevens⁽¹²⁾ is to use small coils, similar to Hemholtz Coils, at various places along the ion path in the magnetic field. These coils have the advantage that the current through them can be varied, thus allowing some "tuning" of the instrument. The following example illustrates the use of this program in planning these methods of aberration correction.

Example: Consider three coils placed at the entrance, the middle, and the exit of the 100-in. mass spectrometer magnet used in the sample problem (p. 12). We wish to find the coil field strengths which will make $B_{11} = 0$ and $|B_{12}| + |B_{22}|$ a minimum. It is convenient to measure the coil field strengths in units of effective boundary radii of curvature, which can be related to the coil currents for a given coil construction. A practical upper limit of coil field strength or minimum radius of curvature may be set at 10 in.

Solution: Since B_{11} , B_{12} , and B_{22} are linear functions of the reciprocals of the coil strengths, they can be written as

$$B_{11} = -\frac{C_1}{R_1} + \frac{C_2}{R_2} + \frac{C_3}{R_3} + C_4;$$

$$B_{12} = \frac{C_5}{R_1} + \frac{C_6}{R_2} + \frac{C_7}{R_3} + C_8;$$

$$B_{22} = \frac{C_9}{R_1} + \frac{C_{10}}{R_2} + \frac{C_{11}}{R_3} + C_{12},$$

where the C's are constants, and R_1 , R_2 , and R_3 are the coil field strengths. To find the C's, set all three R's equal to infinity and obtain C_4 , C_8 , and C_{12} by use of this program. Next, take any three linearly independent sets of (R_1, R_2, R_3) and calculate the B coefficients for each set. This procedure gives three sets of three linear simultaneous equations which can be solved for the nine remaining C's. At this point we have,

$$B_{11} = \frac{71.67}{R_1} + \frac{61.09}{R_2} + \frac{2.981}{R_3} + 0.1805;$$

$$B_{12} = \frac{301.5}{R_1} + \frac{372.7}{R_2} + \frac{20.26}{R_3} - 6.140;$$

$$B_{22} = \frac{317.2}{R_1} + \frac{568.4}{R_2} + \frac{34.42}{R_3} - 9.747.$$

The magnetic field is broken into two separate fields, zero distance apart, for calculating the effects of the middle coil. Setting the B's equal to zero and solving for the R's yields a physically unrealizable result. However, the stated problem of making $B_{11} = 0$ and $|B_{12}| + |B_{22}|$ a minimum, subject to the conditions $|R_1| \geq 10$, can be solved by straightforward linear programming methods.⁽¹³⁾ The solution is $R_1 = -28.912$, $R_2 = 23.528$, $R_3 = -10$, and minimum of $|B_{12}| + |B_{22}| = 2.755$. Other simple synthesis problems can be handled by similar methods.

THE FORTRAN PROGRAM

The program was written in "basic" Fortran through use of the most elementary forms of Fortran statements. All input-output statements are written for cards and are enclosed by lines of asterisks. This program should be easy to adapt to any computer installation. The program running time is negligible, the CDC 3600 machine at Argonne compiled the program in 35 sec and calculated about 120 fields per minute. A program flowchart (Fig. 8) and listing (Table IV) follow.

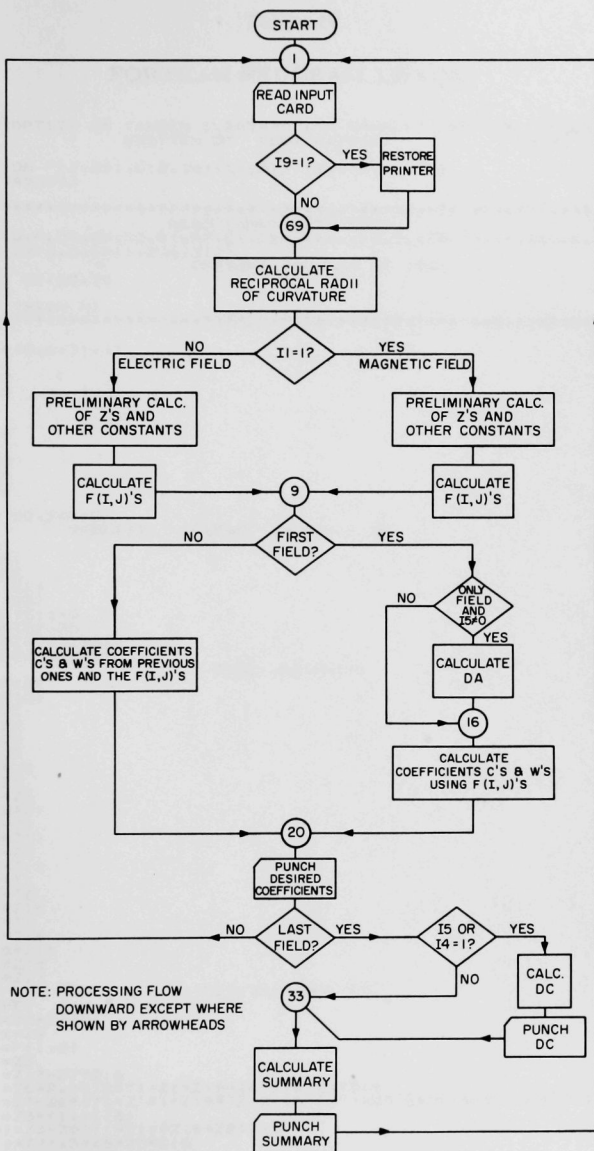


Fig. 8. Fortran Program Flowchart

Table IV

FORTRAN PROGRAM LISTING

C			IOP	001
C			IOP	002
C			IOP	003
C			IOP	004
			IOP	005
			IOP	006
			IOP	007
C			IOP	008
C			IOP	009
			IOP	010
			IOP	011
			IOP	012
			IOP	013
C			IOP	014
			IOP	015
C			IOP	016
C			IOP	017
			IOP	018
			IOP	019
			IOP	020
			IOP	021
			IOP	022
			IOP	023
			IOP	024
			IOP	025
			IOP	026
			IOP	027
			IOP	028
			IOP	029
			IOP	030
C			IOP	031
			IOP	032
			IOP	033
			IOP	034
			IOP	035
			IOP	036
			IOP	037
			IOP	038
			IOP	039
			IOP	040
C			IOP	041
			IOP	042
			IOP	043
			IOP	044
			IOP	045
			IOP	046
			IOP	047
			IOP	048
			IOP	049
			IOP	050
			IOP	051
			IOP	052
			IOP	053
			IOP	054
			IOP	055
			IOP	056
			IOP	057
			IOP	058
			IOP	059
			IOP	060
			IOP	061
			IOP	062
			IOP	063
			IOP	064
C			IOP	065
			IOP	066
			IOP	067
			IOP	068
			IOP	069
			IOP	070
			IOP	071
			IOP	072
			IOP	073
			IOP	074
			IOP	075
			IOP	076
			IOP	077
			IOP	078
			IOP	079
			IOP	080

Table IV (Contd.)

	F(2,1)=Z2+Z1*T2	10P	081
	F(2,2)=-Z1+Z2*(T1+T2)+Z1*Z18	10P	082
	F(2,5)=Z1+Z5*T2	10P	083
	F(2,4)=F(2,2)	10P	084
	F(2,3)=.5*F(2,5)	10P	085
	F(2,6)=Z10+Z12*T2-Z6*Z16+Z3*(P2-.5*Z17)	10P	086
	F(2,7)=2.*Z10*T1+Z6*(T2-Z17-2.*Z19)+Z2*Z15+2.*Z12*Z18-Z13*Z16	10P	087
	1+Z1*Z21-Z3*Z22+2.*P2*(Z6+Z3*T1)	10P	088
	F(2,8)=Z7*(T2+Z15*Z17)-.5*Z4*(Z17+Z21)+Z6*(Z16+Z18-Z20-Z22)	10P	089
	1-Z13*Z19+P2*(Z4+2.*Z6*T1+Z3*Z15)+P1*(Z2+Z1*T2)	10P	090
	F(2,9)=-Z6*T2-Z14*Z16+Z8*(2.*P2-Z17)	10P	091
	F(2,10)=Z1-Z2*T1+(Z3-Z2)*T2-Z16*(2.*Z6-Z1)-Z18*(Z1+Z6)-Z11*Z17	10P	092
	1-Z14*Z19-Z8*Z22+2.*P2*(Z11+Z8*T1)	10P	093
	F(2,11)=-Z1+(Z7-Z5)*T2-Z8*Z16+Z5*Z5*(P2-.5*Z17)	10P	094
	F(2,12)=Z10+Z9*T2	10P	095
	F(2,13)=-2.*Z10*T1+Z9*Z18	10P	096
	F(2,14)=Z10*Z15+Z9*Z21	10P	097
	F(2,15)=1.-Q*T2	10P	098
	F(2,16)=Q*Z18-T1-T2	10P	099
	D0 55 1=1,2	10P	100
	F(1,17)=.5*F(1,9)	10P	101
	F(1,18)=.5*F(1,10)	10P	102
	F(1,19)=.5*F(1,5)+F(1,11)	10P	103
	F(1,20)=.25*F(1,11)-.125*F(1,5)	10P	104
	IF(16) 50,55,58	10P	105
58	F(1,5)=.5*F(1,5)	10P	106
	F(1,9)=F(1,17)	10P	107
	F(1,10)=F(1,18)	10P	108
	F(1,11)=F(1,20)	10P	109
	F(1,19)=.5*F(1,19)	10P	110
55	CONTINUE	10P	111
	GO TO 9	10P	112
C		10P	113
39	A=SQRTF(2.-E1)	10P	114
	Q=PI*Q	10P	115
	G=SQRTF(E1)	10P	116
	F1=Q*G	10P	117
	E2=E1*(1.+E2)	10P	118
	RE=E1*E2	10P	119
	E2=1.+E2	10P	120
	B=3.*E(1-1.)-.5*RE	10P	121
	D=E1+RE	10P	122
	F2=G*A	10P	123
C		10P	124
	Z1=SINF(F2)	10P	125
	Z2=COSF(F2)	10P	126
	Z3=SINF(F1)	10P	127
	Z4=COSF(F1)	10P	128
	Z5=Z2*Z2	10P	129
	Z6=Z4*Z4	10P	130
	Z7=Z1*Z2	10P	131
	Z8=Z3*Z4	10P	132
	Z9=A*A	10P	133
	Z10=3.*Z9	10P	134
	Z11=A*Z10	10P	135
	Z12=Z9*Z9	10P	136
	Z13=3.*Z12	10P	137
	Z14=A*Z13	10P	138
	Z15=B+Z9	10P	139
	Z16=2.*B-Z9	10P	140
	Z17=B-2.*Z9	10P	141
	Z18=2.-3.*E1	10P	142
	Z19=Z18-2.*E1	10P	143
	Z20=Z5*Z17	10P	144
	Z21=3.*F2*(2.*B+Z9+Z12)	10P	145
	Z22=Z1*Z21	10P	146
	Z21=Z2*Z21	10P	147
C		10P	148
	F(1,J) ELECTRIC	10P	149
	F(1,1)=Z1/A	10P	150
	F(1,2)=Z2	10P	151
	F(1,3)=0.	10P	152
	F(1,4)=Z2	10P	153
	F(1,5)=2.*Z1-Z2/Z9	10P	154
	F(1,6)=(Z15-Z2*Z16+Z20)/Z13	10P	155
	F(1,7)=(Z1*Z16-2.*Z7*Z17)/Z11	10P	156
	F(1,8)=(Z16-Z2*Z15-Z5*Z17)/Z10	10P	157
	F(1,9)=(Z13+4.*Z10+Z16)*Z1+4.*Z7*Z17-Z21/Z14	10P	158
	F(1,10)=(4.*(Z20+Z2*Z15-Z16)+Z22)/Z13	10P	159
	F(1,11)=(20.*Z15+Z13-(16.*Z15+4.*Z10+Z13)*Z2-4.*Z20-2.*Z22)	10P	160
	1/(A*Z14)	10P	161
	F(1,12)=(E2*(2.*E1*Z2+Z18-Z6*Z9)/(2.*Z19)+Z2-1.)/Z9	10P	162
	F(1,13)=G*E2*Z8/Z19-Z1*Q/(A*Z19)	10P	163
	F(1,14)=(D*(Z6*Z9-Z2*Z18-2.*E1)/(2.*Z19)+E1*(Z2-1.))/Z9	10P	164
	1.*5*F(1,1)*P1	10P	165
	IF(E1) 10,11,10		

Table IV (Contd.)

11	F(1,15)=0	IOP	166	
	GO TO 12	IOP	167	
10	F(1,15)=Z3/G	IOP	168	
12	F(1,16)=Z4	IOP	169	
	F(2,1)=Z2	IOP	170	
	F(2,2)=-A*Z1	IOP	171	
	F(2,3)=0.	IOP	172	
	F(2,4)=F(2,2)	IOP	173	
	F(2,5)=2.*Z1/A	IOP	174	
	F(2,6)=Z16*(Z1-Z7)/Z11	IOP	175	
	F(2,7)=Z16*(1.+Z2-2.*Z5)/Z10	IOP	176	
	Z7=Z7*Z16	IOP	177	
	F(2,8)=(Z1*Z15+Z7)/(3.*A)	IOP	178	
	F(2,9)=(2.*Z16*(2.*Z5-Z2-1.)+Z22)/Z13	IOP	179	
	F(2,10)=(2.*Z15+Z10+Z13)*Z1-4.*Z7+Z21)/Z11	IOP	180	
	F(2,11)=(4.*Z15+2.*Z10-Z13)*Z1+4.*Z7-2.*Z21)/Z14	IOP	181	
	F(2,12)=F(1,13)-F(1,1)+.5*F(1,15)*F(1,15)*P2	IOP	182	
	F(2,13)=D*(2.*Z6-Z2-1.)/Z19+F(1,15)*F(1,16)*P2	IOP	183	
	F(2,14)=D*(.5*Z1*Z18/A-G*Z8)/Z19-E1*Z1/A+.5*(F(2,1)*P1	IOP	184	
	+F(1,16)*F(1,16)*P2)	IOP	185	
	F(2,15)=Z4	IOP	186	
	F(2,16)=-G*Z3	IOP	187	
	DO 56 I=1,2	IOP	188	
	IF(16) 50,59,60	IOP	189	
60	F(1,5)=.5*F(1,5)	IOP	190	
	F(1,9)=.5*F(1,9)	IOP	191	
	F(1,10)=.5*F(1,10)	IOP	192	
	F(1,11)=.25*F(1,11)-.125*F(1,5)	IOP	193	
59	F(1,17)=0.	IOP	194	
	F(1,18)=0.	IOP	195	
	F(1,19)=0.	IOP	196	
56	F(1,20)=0.	IOP	197	
9	IF(K1-1) 50,13,14	IOP	198	
C		FIRST FIELD SUBPROGRAM	IOP	199
13	IF(K2-1) 50,15,16	IOP	200	
15	IF(15) 50,16,17	IOP	201	
17	A=F(1,2)+F(2,1)	IOP	202	
	DA=R*(-A-SQRTF(A*A-4.*F(1,1)*F(2,2)))/(2.*F(2,2))	IOP	203	
16	DA=DA/R	IOP	204	
	DS=DA*DA	IOP	205	
	DO 18 I=1,2	IOP	206	
	C(1,1)=F(1,1)+F(1,2)*DA	IOP	207	
	C(1,2)=F(1,5)	IOP	208	
	C(1,3)=F(1,3)	IOP	209	
	C(1,4)=F(1,4)	IOP	210	
	C(1,5)=F(1,15)+F(1,16)*DA	IOP	211	
	C(1,6)=F(1,16)	IOP	212	
	C(1,7)=F(1,6)+F(1,7)*DA+F(1,8)*DS	IOP	213	
	C(1,8)=F(1,9)+F(1,10)*DA	IOP	214	
	C(1,9)=F(1,11)	IOP	215	
	C(1,10)=F(1,17)+DA*F(1,18)	IOP	216	
	C(1,11)=F(1,19)	IOP	217	
	C(1,12)=F(1,20)	IOP	218	
	C(1,13)=F(1,7)+2.*F(1,8)*DA	IOP	219	
	C(1,14)=F(1,10)	IOP	220	
	C(1,15)=F(1,8)	IOP	221	
	C(1,16)=F(1,12)+F(1,13)*DA+F(1,14)*DS	IOP	222	
	C(1,17)=F(1,13)+2.*F(1,14)*DA	IOP	223	
18	C(1,18)=F(1,14)	IOP	224	
	RB=R	IOP	225	
	W(1,1)=DA*R	IOP	226	
	W(1,2)=0.	IOP	227	
	W(1,3)=0.	IOP	228	
	W(1,4)=1.	IOP	229	
	W(1,5)=DA*R	IOP	230	
	W(1,6)=1.	IOP	231	
DO 61 J=1,6		IOP	232	
61	W(2,J)=R*C(1,J)	IOP	233	
	W(2,4)=W(2,4)/R	IOP	234	
	W(2,6)=W(2,6)/R	IOP	235	
C		IOP	236	
	*****	IOP	237	
	PUNCH COEFFICIENT PRINT OR RAY TRACE	IOP	238	
30	FORMAT(///)	IOP	239	
19	FORMAT(/4X2H RI2,4F18.8/(8X4F18.8))	IOP	240	
65	PUNCH 30	IOP	241	
20	IF(17) 50,62,37	IOP	242	
37	PUNCH 52,41((C(1,J),J=1,18),I=1,2)	IOP	243	
52	FORMAT(/4X2H CI2,4F18.8,3/(8X4F18.8)/8X2F18.8,/(8X4F18.8))	IOP	244	
62	IF(18) 50,21,41	IOP	245	
41	PUNCH 19,K1,((W(1,J),J=1,6),I=1,2)	IOP	246	
	*****	IOP	247	
C		IOP	248	
21	RA=R	IOP	249	
	IF(K2-K1) 50,23,1	IOP	250	

Table IV (Contd.)

		MORE THAN 1 FIELD COMBINATION SUBPROGRAM			
C	14	DO 44 J=1,6		IOP	251
		W(1,J)=R*C(1,J)+DB*C(2,J)		IOP	252
		IF(13) 50,44,82		IOP	253
	82	IF(J-5) 83,44,44		IOP	254
	83	W(1,J)=-W(1,J)		IOP	255
	44	CONTINUE		IOP	256
		W(1,4)=W(1,4)/RB		IOP	257
		W(1,6)=W(1,6)/RB		IOP	258
		U=RA/R		IOP	259
		V=DB/R		IOP	260
		DO 24 J=1,18		IOP	261
	24	S(J)=U*C(1,J)+V*C(2,J)		IOP	262
		IF(13) 50,25,26		IOP	263
	26	DO 27 I=1,2		IOP	264
		F(1,1)=-F(1,1)		IOP	265
		F(1,2)=-F(1,2)		IOP	266
		F(1,9)=-F(1,9)		IOP	267
		F(1,10)=-F(1,10)		IOP	268
		F(1,17)=-F(1,17)		IOP	269
	27	F(1,18)=-F(1,18)		IOP	270
	25	D1=C(2,1)		IOP	271
		D2=C(2,2)		IOP	272
		D3=C(2,3)		IOP	273
		D4=C(2,4)		IOP	274
		H3=C(2,5)		IOP	275
		H4=C(2,6)		IOP	276
		DO 28 I=1,2		IOP	277
		DO 28 J=1,18		IOP	278
	28	T(1,J)=F(1,1)*C(2,J)+F(1,2)*S(J)		IOP	279
		DO 29 I=1,2		IOP	280
		C(1,1)=T(1,1)		IOP	281
		C(1,2)=T(1,2)+F(1,5)		IOP	282
		C(1,3)=T(1,3)+F(1,3)		IOP	283
		C(1,4)=T(1,4)		IOP	284
		C(1,5)=F(1,15)*H3+F(1,16)*S(5)		IOP	285
		C(1,6)=F(1,15)*H4+F(1,16)*S(6)		IOP	286
		C(1,7)=T(1,7)+F(1,6)*D1*D1+F(1,7)*D1*S(1)+F(1,8)*S(1)*S(1)		IOP	287
		C(1,8)=T(1,8)+2.*F(1,6)*D1*D2+F(1,7)*D1*S(2)+D2*S(1)		IOP	288
	1+2.	*F(1,8)*S(1)*S(2)+F(1,9)*D1*D1+F(1,10)*S(1)		IOP	289
		C(1,9)=T(1,9)+F(1,6)*D2*D2+F(1,7)*D2*S(2)+F(1,8)*S(2)*S(2)		IOP	290
	1+F(1,9)*D2+F(1,10)*S(2)+F(1,11)			IOP	291
		C(1,10)=T(1,10)+2.*F(1,6)*D1*D3+F(1,7)*(D1*S(3)+D3*S(1))		IOP	292
	1+2.	*F(1,8)*S(1)*S(3)+F(1,17)*D1+F(1,18)*S(1)		IOP	293
		C(1,11)=T(1,11)+2.*F(1,6)*D2*D3+F(1,7)*(D2*S(3)+D3*S(2))		IOP	294
	1+2.	*F(1,8)*S(2)*S(3)+F(1,9)*D3+F(1,10)*S(3)+F(1,19)		IOP	295
	2+F(1,17)*D2+F(1,18)*S(2)			IOP	296
		C(1,12)=T(1,12)+F(1,6)*D3*D3+F(1,7)*D3*S(3)+F(1,8)*S(3)*S(3)		IOP	297
	1+F(1,17)*D3+F(1,18)*S(3)+F(1,20)			IOP	298
		C(1,13)=T(1,13)+2.*F(1,6)*D1*D4+F(1,7)*(D1*S(4)+D4*S(1))		IOP	299
	1+2.	*F(1,8)*S(1)*S(4)		IOP	300
		C(1,14)=T(1,14)+2.*F(1,6)*D2*D4+F(1,7)*(D2*S(4)+D4*S(2))		IOP	301
	1+2.	*F(1,8)*S(2)*S(4)+F(1,9)*D4+F(1,10)*S(4)		IOP	302
		C(1,15)=T(1,15)+F(1,6)*D4*D4+F(1,7)*D4*S(4)+F(1,8)*S(4)*S(4)		IOP	303
		C(1,16)=T(1,16)+F(1,12)*H3*H3+F(1,13)*H3*S(5)+F(1,14)*S(5)*S(5)		IOP	304
		C(1,17)=T(1,17)+2.*F(1,12)*H3*H4+F(1,13)*(H3*S(6)+H4*S(5))		IOP	305
	1+2.	*F(1,14)*S(5)*S(6)		IOP	306
	29	C(1,18)=T(1,18)+F(1,12)*H4*H4+F(1,13)*H4*S(6)+F(1,14)*S(6)*S(6)		IOP	307
		DO 47 J=1,6		IOP	308
	47	W(2,J)=R*C(1,J)		IOP	309
		W(2,4)=W(2,4)/RB		IOP	310
		W(2,6)=W(2,6)/RB		IOP	311
		GO TO 20		IOP	312
C			SUMMARY	IOP	313
	23	S(1)=-RA*C(1,5)/C(2,5)		IOP	314
		S(3)=1./C(2,1)		IOP	315
		S(4)=1./C(2,5)		IOP	316
		IF(15) 50,32,31		IOP	317
	32	IF(14) 50,33,31		IOP	318
	31	DC=-RA*C(1,1)/C(2,1)		IOP	319
C		*****		IOP	320
C		PUNCH DC		IOP	321
C		PUNCH DC		IOP	322
C		PUNCH 34,DC		IOP	323
C		34 FORMAT(/4X4H DC F18.8)		IOP	324
C		*****		IOP	325
C		*****		IOP	326
	33	DO 64 J=1,6		IOP	327
	64	T(1,J)=R*C(1,J)+DC*C(2,J)		IOP	328
		T(1,4)=T(1,4)/RB		IOP	329
		T(1,6)=T(1,6)/RB		IOP	330
		DC=DC/RA		IOP	331
		S(7)=C(1,3)+DC*C(2,3)		IOP	332
		S(8)=C(1,10)+DC*C(2,10)		IOP	333
		S(9)=C(1,11)+DC*C(2,11)		IOP	334
				IOP	335

Table IV (Contd.)

	IF(S(8)) 53,54,53	IOP	336
54	S(5)=90.	IOP	337
	S(6)=90.	IOP	338
	GO TO 57	IOP	339
53	S(5)=ATANF(-C(2,1)*S(7)/S(8))/PI	IOP	340
	S(6)=ATANF(-C(2,2)*S(7)/S(9))/PI	IOP	341
57	DO 35 J=1,18	IOP	342
35	C(1,J)=C(1,J)+DC*C(2,J)	IOP	343
	S(2)=RA*C(1,3)	IOP	344
C	*****	IOP	345
C	PUNCH SUMMARY	IOP	346
	66 FORMAT(/4X4H RS 4F18.8/8X2F18.8)	IOP	347
	67 FORMAT(/4X4H S1 4F18.8/(8X4F18.8))	IOP	348
	68 FORMAT(/4X4H S2 4F18.8/8X2F18.8)	IOP	349
	IF(18) 50,51,49	IOP	350
49	PUNCH 66,(T(1,J),J=1,6)	IOP	351
51	PUNCH 67,(C(1,J),J=1,18)	IOP	352
	PUNCH 68,(S(J),J=1,6)	IOP	353
C	*****	IOP	354
	GO TO 1	IOP	355
50	STOP	IOP	356
	END	IOP	357
		IOP	358
		IOP	359

REFERENCES

1. E. G. Johnson and A. O. Nier, Angular Aberrations in Sector Shaped Electromagnetic Lenses for Focusing Beams of Charged Particles, Phys. Rev. 91, 10 (1953).
2. H. G. Voorhies, Second-order Aberrations in Sector Shaped Electro-magnetic Analyzers, Rev. Sci. Instr. 26, 716-717 (1955); 27, 58 (1956).
- 3a. L. A. König and H. Hintenberger, Über die Abbildungsfehler von beliebig begrenzten homogenen magnetischen Sektorenfeldern, Z. Naturforsch. 12a, 377-385 (1957).
- 3b. H. Hintenberger and L. A. König, Mass Spectrometers and Mass Spectrographs Corrected for Image Defects, Advances in Mass Spectrometry (Ed. by J. D. Waldron), Pergamon Press (1959).
- 4a. H. Ewald and H. Liebl, Die Bildfehler des Toroidkondensators, Z. Naturforsch. 12a, 28-33, 588 (1957).
- 4b. H. Liebl, Die Schnittwinkel der Richtungs- und Energiefokussierungskurven bei doppelfokussierenden Massenspektrographen, Optik 16, 19-26 (1959).
- 5a. H. A. Tasman, A. J. H. Boerboom, and H. Wachsmuth, Calculation of the Ion Optical Properties of Inhomogeneous Magnetic Sector Fields, Z. Naturforsch. 14a, 121-129, 816-827 (1959).
- 5b. H. A. Tasman, Ion Optics of Mass Spectrometers with Virtually Enlarged Radius, PhD. Thesis, Leiden (1961).
6. H. A. Tasman, op. cit., 5b, 64-66.
7. R. Albrecht, Das Potential in doppelt gekrümmten Kondensatoren, Z. Naturforsch. 11a, 156-163 (1956).
8. H. A. Tasman, op cit., 5b, Ch. 7. H. Hintenberger and L. A. König, op. cit., 3b: H. Liebl and H. Ewald, Z. Naturforsch. 14a, 199-200 (1959).
9. R. Herzog, Ablekung von Kathoden- und Kanalstrahlen am Rande eines Kondensators, dessen Streufeld durch eine Blende begrenzt ist, Z. Physik 97, 596-602 (1935).
10. N. D. Coggeshall and M. Muskat, The Paths of Ions and Electrons in Non-uniform Magnetic Fields, Phys. Rev. 66, 187-198 (1944).
11. S. J. Balestrini and F. A. White, Workable Magnetic Shim to Correct Second-order Aberration in a Mass Spectrometer, Rev. Sci. Instr. 31, 633-636 (1960).
12. C. Stevens, Correction Coils for Second-order Focusing with the Argonne 100 inch Radius Mass Spectrometer, Paper No. 48, meeting of ASTM Committee E-14 on Mass Spectrometry, June 1962.
13. A good introduction to this subject is given in the book by G. Hadley, Linear Programming, Addison-Wesley (1962).

ARGONNE NATIONAL LAB WEST



3 4444 00009054 8